

**CORRELATING CARDIAC ACTION POTENTIALS WITH METABOLIC
MARKERS DURING ACUTE CARDIAC ISCHEMIA IN RABBIT HEARTS**

by
Jeremiah Kimball

A thesis submitted to the faculty of the University of North Carolina at Chapel Hill in
partial fulfillment of the requirements for the degree of Master of Science in the
Department of Biomedical Engineering.

Chapel Hill
2006

Approved by

Advisor: Dr. Stephen B. Knisley

Reader: Dr. Jeffrey Macdonald

Reader: Dr. Caterina Gallippi

ABSTRACT

JEREMIAH KIMBALL: Correlating Cardiac Action Potentials with Metabolic Markers during Acute Cardiac Ischemia in Rabbit Hearts
(Under the direction of Stephen B. Knisley, Ph.D.)

We have developed the first system, to our knowledge, that simultaneously measures ^{31}P nuclear magnetic resonance (NMR) and optical action potentials (APs) in order to determine the dynamic relationship between certain metabolic markers and AP morphology during acute ischemia in rabbit hearts. Our system utilizes a ratiometric optical technique with transmembrane voltage-sensitive dye, di-4-ANEPPS, to measure APs with no pharmacological motion inhibition. Fiber optics measure APs by passing light to and from the heart within an NMR magnet. ^{31}P NMR measurements verified the stoichiometric relationship between inorganic phosphate and phosphocreatine; as phosphocreatine levels decrease, inorganic phosphate levels increase. During acute ischemia, intracellular pH levels remained constant and β -ATP levels decreased 22.4%. Simultaneous optical measurements show reductions in AP amplitude (-83.3%) and heart rate (-56.6%). AP duration increased (+875%), implicating other possible factors. These findings demonstrate a real-time correlation between ischemic depletion of high-energy phosphagens, and decreased AP amplitude and duration.

ACKNOWLEDGMENTS

I would like to thank everyone that was involved in helping me to complete this research project. First and foremost, I would like to thank Dr. Stephen B. Knisley for his guidance, motivation, support, and expertise throughout the term of this research. Thank you also to Dr. Jeffrey Macdonald from the UNC-CH Department of Biomedical Engineering. I would also like to thank Arielle Drummond for her previous work on the project. Thanks to Marc ter Horst from the UNC-CH Department of Chemistry for the training and support concerning the NMR equipment. I would also like to thank Dr. Caterina Gallippi (two l's and two p's) for all her time and support as part of my Masters Committee. Thanks also to John Dumas and Denny Himel, Ph.D. candidates under Dr. Knisley, for their help on the project.

TABLE OF CONENTS

	Page
LIST OF FIGURES.....	vi
LIST OF TABLES.....	vii
LIST OF ABBREVIATIONS.....	viii
Chapter	
I INTRODUCTION.....	1
II BACKGROUND.....	3
2.1 - Overview.....	3
2.2 - Cardiac Ischemia and Its Effects on Action Potentials and Metabolism.....	3
2.3 - Fluorescence and Ratiometry Overview.....	7
2.4 - ³¹ P NMR Overview.....	9
III METHODS.....	12
3.1 - Optimization of the Dual Modality System.....	12
3.2 - Heart Preparation.....	13
3.3 - ³¹ P NMR and Optical Fluorescence Measurements.....	15
IV RESULTS.....	18
4.1 – Overview.....	18
4.2 - Optical Recordings in Control, Ischemia, and Reperfusion.....	18

4.3 - ^{31}P NMR Spectroscopy Recordings in Control, Ischemia, and Reperfusion.....	22
4.4 - Time Course of Phosphates and Intracellular pH.....	24
V DISCUSSION.....	27
5.1 - Explanations for Abnormal Optical AP Morphology.....	27
5.2 - Viability of AP Recordings.....	29
5.3 - Simultaneous ^{31}P NMR and Optical Recordings of APs.....	32
VI CONCLUSIONS.....	34
REFERENCES.....	35

LIST OF FIGURES

Figure 2.1:	Simplified Ventricular Cardiac Myocyte AP.....	4
Figure 2.2:	Shift in wavelength of Di-4-ANEPPS in response to changes in cardiac myocyte transmembrane voltage.....	9
Figure 3.1:	Diagram of the perfusion apparatus used in rabbit experiments.....	14
Figure 3.2:	Optical recording system for ratiometric measurements in rabbit hearts stained with transmembrane voltage- sensitive fluorescent dye di-4-ANEPPS.....	16
Figure 4.1:	Ratiometric fluorescence recordings of action potentials (A) during pre-ischemia of Run #1 and (B) at key points during Run #2.....	19
Figure 4.2:	Implementation of the 5ms boxcar filter.....	20
Figure 4.3:	Representative ³¹ P NMR spectra from Run #1.....	23
Figure 4.4:	Complete time course of changes in β-ATP, PCr, and Pi levels during (A) Run #1 and (B) Run #2.....	25
Figure 4.5:	Complete time course of changes in intracellular pH during (A) Run #1 and (B) Run #2.....	26
Figure 5.1:	Fluorescence emission recordings for (A) Run #1 (pre-ischemia) and (B) Run #2 (approx. 4 min into ischemia).....	31

LIST OF TABLES

Table 3.1:	^{31}P NMR Parameters for Maximum Temporal Resolution.....	12
Table 4.1:	Optical Action Potential Analysis for Run #2.....	21

LIST OF ABBREVIATIONS

VF	ventricular fibrillation
NMR	nuclear magnetic resonance spectroscopy
AP	action potential
mM	millimolar
ml	milliliter
nm	nanometer
ppm	part per million
Hz	hertz
μsec	microsecond
sec	second
min	minute
dB	decibel
TD	number of data points
NS	number of scans
DS	number of dummy scans
SW	sweep width
AQ	acquisition time
D1	pre-acquisition delay or relaxation time
P1	pulse width
PL1	power level
FID	free induction decay
PBS	phosphate buffered saline

SNR	signal-to-noise ratio
PMT	photomultiplier tube
PH0	zero-order phasing
ABS	automatic baseline subtraction
PME	phosphomonoesters
APA	action potential amplitude
APD _{50%}	action potential duration at 50% amplitude
BPM	heartbeats per minute
ATP	adenosine triphosphate
% TP	percent total phosphate
EAD	early afterdepolarization
DAD	delayed afterdepolarization
°C	degrees Celsius
Na ⁺	sodium ion
Ca ²⁺	calcium ion
K ⁺	potassium ion
Mg ²⁺	magnesium ion
³¹ P	phosphorous-31
RF	radiofrequency
B ₀	large, constant applied magnetic field
B ₁	local, short duration magnetic field

CHAPTER I

INTRODUCTION

^{31}P nuclear magnetic resonance spectroscopy (NMR) has long been shown effective in measuring the concentrations of key high energy phosphate compounds involved in cardiac metabolism (Gadian DG et. al. 1976; Marsden PK et. al. 2000; Honda H et. al. 2002). By collecting time-resolved ^{31}P NMR spectra, changes in these metabolic marker concentrations can be analyzed through time. Cardiac ischemia, the blockage or constriction of coronary arteries, has frequently been the subject of such studies. Simultaneous measurement of metabolic marker concentrations with cardiac transmembrane action potentials (APs) would allow greater insight into possible mechanisms behind changes in AP morphology during cardiac ischemia.

Early measurements of cardiac APs utilized microelectrodes, however, these systems incorporate metal components that might interfere with NMR spectroscopy measurements or vice-versa. With the development of a ratiometric optical technique for measuring cardiac APs with no pharmacological motion inhibition, simultaneous measurement of cardiac APs and metabolic marker levels is possible. Dual modality systems have been utilized for decades to correlate different functional aspects of cardiac dysfunction (Tamura, H et al. 1988; Tamura, H et al. 1989; Kupriyanov, D et al. 2000; Marsden, S et al. 2002). No other technique is known to simultaneously utilize ^{31}P NMR and optical AP recordings with ratiometry to correlate high energy phosphagen levels and

transmembrane potentials in the heart. The potential benefits for a real-time system for imaging biochemical activity within the heart seem applicable to some forms of heart disease.

Prior to this thesis, the novel dual modality system to simultaneously measure cardiac APs and high energy metabolites was fabricated. This thesis concerns the optimization of that system and utilizing it to determine the dynamic relationship between AP morphology and certain metabolic marker levels during acute ischemia. Five high energy metabolites were observed over the time course of these measurements including pH, sugar phosphates, phosphocreatine, phospholipid intermediates, and ATP. This novel system and the important information it provides will join on-going research to determine the effects of cardiac ischemia and how ischemia can lead to an increased defibrillation threshold and arrhythmias.

CHAPTER II

BACKGROUND

2.1 Overview

Cardiac arrest is the sudden loss of cardiac function resulting from the cessation of all rhythmical impulses in the heart (Guyton AC and Hall JE 2000). Even though it is currently the focus of a substantial amount of research, the mechanisms behind what causes cardiac arrest are not completely understood. Initial symptoms may include chest pains, but late stages without treatment irrevocably lead to unconsciousness, loss of pulse and respiration, and death. A common cause of cardiac arrest is ventricular fibrillation (VF) (Zipes DP and Jalife J 2000). In VF, sudden rapid, erratic electrical activity in the ventricles of the heart leads to the loss of coordinated contractions of the heart. Heartbeats are rapid and inefficient leading to the cessation of blood circulation in the body. Cardiac ischemia, the lack of oxygenated blood flow to myocardial tissues, often leads to arrhythmias such as VF (Penny, W.J. et al. 1983). Therefore, understanding the effects of cardiac ischemia, how they lead to VF and the development of treatment methods, is a very important area of research.

2.2 Cardiac Ischemia and Its Effects on Action Potentials and Metabolism

Cardiac ischemia is caused by the blockage or constriction of coronary arteries. This reduction in oxygenated blood flow to myocardial tissue can cause irreversible damage to the heart if prolonged. Reperfusion, the return of oxygenated blood flow,

might seem like the end solution to acute cardiac ischemia; however, even reperfusion can cause more injury to the heart (Braunwald E. et. al. 1985).

Cardiac muscle contractions are the result of rhythmic, coordinated electrical activity. Electrical stimulation of cardiac muscle usually begins at the sinoatrial node, the impulse generating (pacemaker) tissue located in the right atrium of the heart. This electrical impulse, or action potential (AP), propagates throughout the heart via a specialized conduction system. APs serve to stimulate the excitatory and conductive muscle fibers of the heart to induce contractions. APs begin with rapid changes in membrane potential, usually from resting level between -80 mv and -90 mv, then becoming positive 40mv. The threshold for sodium current activation during the beginning of an AP is generally considered to be approximately -65 mv (Zipes DP and Jalife J 2000). Figure 2.1 illustrates the simplified shape of an AP generated by a ventricular cardiac myocytes.

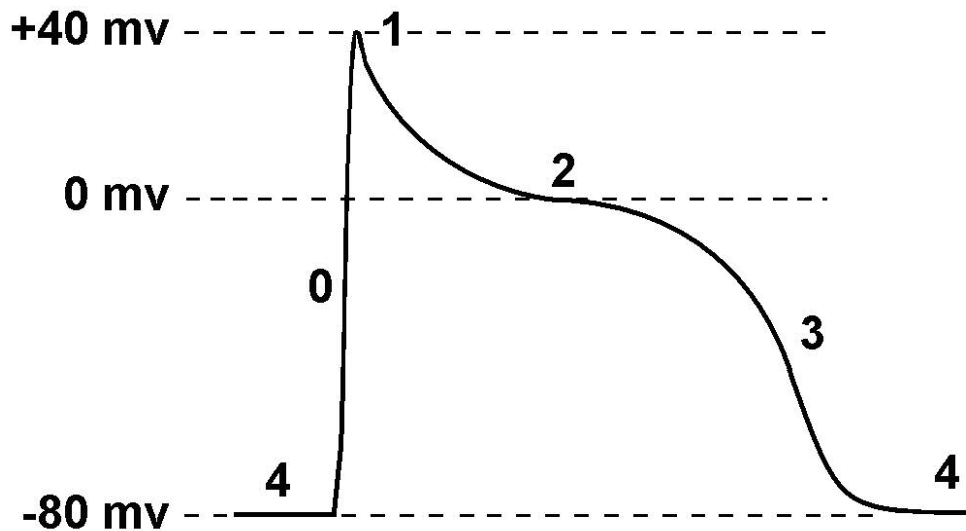


Figure 2.1. *Simplified Ventricular Cardiac Myocyte AP.*

The cardiac AP has five sections or phases. Phase 4 represents resting membrane potential. Phase 0, the upstroke, represents rapid depolarization; this results in the

opening of some voltage-gated Na^+ channels, the rapid influx of Na^+ , and further depolarization. This causes the remainder of the voltage gated Na^+ channels to open and further depolarization. Phase 1 begins once a membrane potential of approximately +40 mv is reached. At this point, the voltage-gated Na^+ channels become inactivated; simultaneously, voltage-gated potassium channels begin to open, causing a slight repolarization. During phase 2, the plateau, L-type (“long-lasting”) voltage-gated Ca^{2+} channels open creating a momentary balance between Ca^{2+} influx and K^+ efflux. Phase 3 represents the inactivation of the L-type Ca^{2+} channels and continued efflux of K^+ , repolarizing the cell. Voltage-gated K^+ channels become inactivated around -45 mv, but K^+ efflux continues through K^+ leakage channels until resting membrane potential is reached (Guyton, A. C. et. al. 2000).

During ischemia, the ion concentrations of cardiac myocytes (cardiac muscle cells) change. Extracellular potassium concentrations increases as a result of three factors: ATP-dependent K^+ channel activation causing an efflux of potassium (Taniguchi, J. et. al. 1983), a reduction in Na^+ - K^+ pump activity causing a decrease in K^+ influx (Weiss, J., et. al. 1986), and a decrease in extracellular space due to the increase in osmotically active particles inside the cell (Tranum-Jensen, J. et. al. 1981). Intracellular sodium concentrations typically increase as a result of passive inward leakage and reduced active efflux (Carmeliet, Edward. 1999). This may be a partial result of an increase in intracellular magnesium ions, due to accelerated ATP hydrolysis, which block sodium efflux from Na^+ / Mg^{2+} channels (De Weer, P. 1976). Intracellular calcium tends to increase and “overload” during cardiac ischemia due to four factors: less efficient removal to the extracellular space, reduced sarcoplasmic reticulum (SR) uptake,

increased inward leak, and displacement by H⁺ from binding sites (Peuhkurinen, K. J. 2000). Increased calcium overload can cause spontaneous calcium release in the absence of trigger Ca²⁺. The result can be early afterdepolarizations (EAD) and/or delayed afterdepolarizations (DAD) (Luo, Ching-Hsing. et al. 1994).

These changes in ion concentrations seem to be a major factor behind changes in AP morphology. Acute ischemia results in a depolarization from the normal resting membrane potential, producing a transient increase in excitability. Depending on the extent of further depolarization, fast Na⁺ current is either partially or completely inhibited. This, along with the rise in extracellular potassium, leads to the depression of AP amplitude and upstroke velocity (Carmeliet, Edward. 1999; Coronel, R. et al. 1989). AP duration is initially prolonged, but begins to shorten soon afterwards due partially to rising extracellular potassium levels (Verkerk, Arie O., Veldkamp, Marieke W., et al. 1996). On a larger scale, these changes tend to cause a decrease in heart rate as ischemia progresses. Most of the normal AP morphological features recover during reperfusion after acute ischemia; however, coronary vascular injury and the no-reflow phenomenon due to oxygen radical stress can cause abnormal AP morphology during reperfusion, especially concerning AP duration (Aiello, Ernesto A. et al. 1995).

Ischemia also causes major disturbances in myocardial metabolism. High-energy phosphate metabolite levels experience abnormal fluctuations due to the lack of oxygenated blood flow. Any oxygen remaining in the system is consumed by oxidative phosphorylation. Phosphocreatine (PCr) stores are consumed to maintain a steady production of ATP, the body's principal source of energy; however these reserves are not limitless. They can become exhausted with prolonged ischemia. Inorganic phosphate (Pi)

levels rise due to the consumption of ATP and the inability of the tissues to regulate metabolic waste accumulation. Anaerobic metabolism (glycolysis) is initiated, but can only help maintain ATP levels for a short period of time due limited ATP production efficiency and the buildup of lactic acid and hydrogen ions. If ischemia is prolonged, ATP levels will begin to drop dramatically (Peuhkurinen, K. J. 2000). Net hydrogen ion concentration rises due to the increased production of protons and insufficient removal (Dennis, S. C. et al. 1991). Increased net hydrogen ion concentration decreases intracellular pH, causing acidosis. Acidosis is known to cause a decrease in resting potential, depressed upstroke velocity, an increase in AP duration, and possibly EADs; however, prolongation of the AP and EADs are not seen during ischemia (Coraboeuf, E. et. al. 1980).

2.3 Fluorescence and Ratiometry Overview

A photon is a unit or “particle” of electromagnetic radiation. Photons have a unique wavelength that is inversely proportional to their energy. Therefore, higher energy photons have shorter wavelengths, i.e. red light at 650 nm has more energy than green light at 420 nm. Fluorescence is the emission of electromagnetic radiation in which a molecule absorbs a high-energy photon, and re-emits it as a lower-energy photon. Molecules that carry fluorescent properties are called fluorophores or fluorescent dyes.

When a fluorophore is irradiated with a photon of light at the appropriate excitation wavelength, the photon is absorbed. This process creates an excited state where the fluorophore undergoes certain conformational changes. Shortly thereafter, the molecules excited by absorption return to their ground state, emitting a photon in the

process. The photon emitted is of a lesser energy (longer wavelength) than the photon absorbed due to the energy loss encountered over the course of the interaction.

Di-4-ANEPPS is a fast, voltage-sensitive, fluorescent dye commonly used to detect action potentials across the membranes of cardiac muscle cells (myocytes). Di-4-ANEPPS is unique because its structure allows it to anchor into the membrane of a muscle cell. When excited by visible light of suitable wavelength, i.e. blue laser light at 488 nm, it emits a combination of red and green light. However, if placed inside a cardiac myocyte cell membrane, it will experience a reversible shift towards shorter wavelengths in response to membrane depolarization (Fluhler, E. et. al. 1985). In the case of excitation by blue laser light at 488 nm, depolarization will shift emission towards wavelengths associated with green light (510-570 nm), increasing green light intensity. Also advantageous is the fact that the increase in green emission during depolarization is directly proportional to the simultaneous decrease in red (>590 nm) emission (Johnson, P.L. et. al. 1999). Figure 2.2 illustrates the reversible shift of Di-4-ANEPPS in response to changes in transmembrane voltage.

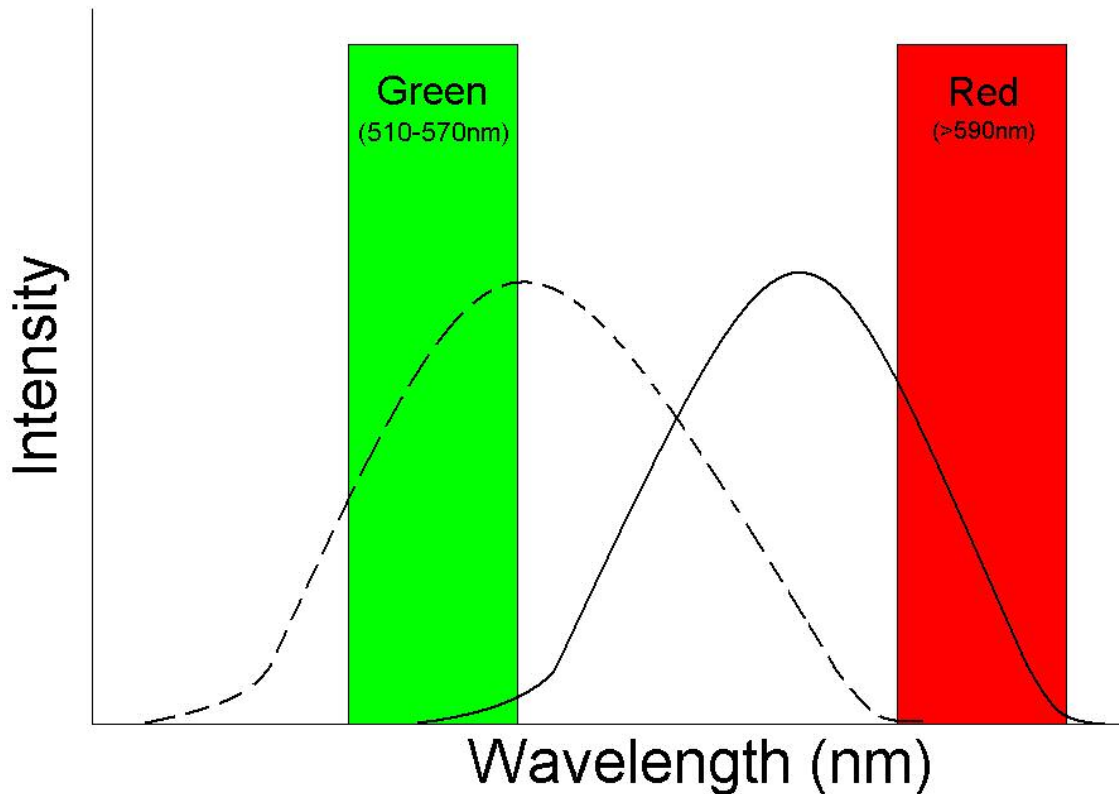


Figure 2.2. Shift in wavelength of Di-4-ANEPPS in response to changes in cardiac myocyte transmembrane voltage. The broken line represents shift in wavelength due to depolarization.

The advantage of using Di-4-ANEPPS to measure changes in cardiac myocyte transmembrane voltage is the ability to record both red and green emissions for the purpose of using their ratio to reveal the true optical action potential. By taking the ratio of green to red emissions, changes in fluorescence common to both signals cancel; therefore, the effects of motion, photobleaching, and variations in dye concentration are significantly lessened (Knisley, S.B. et al. 2000).

2.4 ³¹P NMR Overview

Nuclear magnetic resonance spectroscopy (NMR) exploits the magnetic properties of certain atomic nuclei. Certain nuclei, such as phosphorous-31 (³¹P), possess an intrinsic magnetic moment, associated with its atomic spin. For example, if a strong, homogenous magnetic field, were applied to such nuclei, these tiny “magnets” would

align themselves along the length of the field. NMR allows identification of individual atoms contained within molecules of a sample. In ^{31}P NMR, molecules containing phosphorous can be individually identified by chemical shift based on their unique molecular structure.

There are five units necessary for NMR spectroscopy: the transmitter, magnet, probe, receiver, and computer. The sample is placed inside the probe, centered about the “sweet spot,” the position of best energy propagation efficiency, of the coil of wire. The coil is the main component of the probe considering it is both transmits and receives the radiofrequency energy necessary to produce a signal. The probe is then placed inside the electromagnet that produces a strong, homogenous magnetic field, B_0 , about the probe. The transmitter then transmits a short pulse of power into the probe in the form of a radiofrequency (RF) magnetic field, B_1 , with a frequency corresponding to the resonance frequency. The resonance frequency is unique and depends on the nuclei and B_0 . The coil then applies the RF pulse to the sample and the tiny “magnets,” previously aligned with the large B_0 field, almost instantaneously align with the local B_1 magnetic field. Once the short B_1 pulse dissipates, the nuclei begin to relax back to their original alignment within B_0 . As relaxation progresses, the nuclei emit RF energy that is absorbed by the coil and transmitted to the receiver, where it is collected and sent to the computer for processing.

Depending on the molecular environment of each ^{31}P nuclei within the sample, nuclei will produce signals with slightly different resonance frequencies. For example, ^{31}P nuclei from PCr will appear at a different frequency than the ^{31}P nuclei from ATP. The difference between the resonance frequencies and a standard ^{31}P resonance

frequency reference is called chemical shift and can be in units of parts per million (ppm) or hertz (Hz). These signals are processed by the computer and displayed in the form of NMR spectra. In general, the individual heights of the peaks on NMR spectra correspond to the number of nuclei that contribute to them. Examples of NMR spectra follow in the Results Chapter in Figure 4.3.

CHAPTER III

METHODS

3.1 Optimization of the Dual Modality System

Before performing live rabbit heart experiments, the NMR parameters needed to be optimized for increased temporal resolution. Previously, the original parameters dictated 10 minutes between each spectral acquisition. In order to observe the finer details of rapid changes in AP morphology and high energy metabolite levels, the temporal resolution needed to be increased. To do so, a new set of parameters were introduced (Table 3.1).

Parameter	Value
TD	8192
NS	64
DS	2
SW	56 ppm
AQ (TD/SW)	0.5014004 sec
D1	1.5 sec
P1	50 μ sec

Table 3.1. ³¹P NMR Parameters for Maximum Temporal Resolution

The number of data points (TD) and sweep width (SW) were altered to produce a new, faster acquisition time (AQ). The number of dummy scans (DS), the number of scans (NS), the relaxation time (D1), and pulse width (P1) were all reduced as well. Incorporating these new values provided near maximum temporal efficiency and only 2 minutes per spectral acquisition. All other parameters remained unaltered.

Along with changes to the temporal resolution, the shim set was also improved upon. The shim set is what determines the homogeneity of the magnetic field surrounding the sample. A better shim set will produce a better signal-to-noise ratio (SNR). To imitate the general shape, size, and phosphate composition of a rabbit heart, a small balloon filled with a comparable concentration of phosphate buffered saline (PBS) was placed inside the NMR tube. The shim set was altered by observing changes in the shape of the free induction decay (FID) during a continuous acquisition. Once a potential shim set was produced, spectra were acquired and the SNR was determined. The shim set that produced the best SNR was used during the live rabbit experiments.

3.2 Heart Preparation

Hearts were excised rapidly from pentobarbital-anesthetized New Zealand White rabbits in accordance with Institutional Animal Care and Use Committee guidelines. A cannula including a fiber optic was immediately placed into the aorta with the fiber tip positioned in the left ventricle. The hearts were Langendorff-perfused to flush the blood from the vessels and oxygenate the myocardium. Figure 3.1 illustrates the perfusion apparatus and the components used such as the pump, filter, bubble trap, fiber optic, NMR magnet, etc.

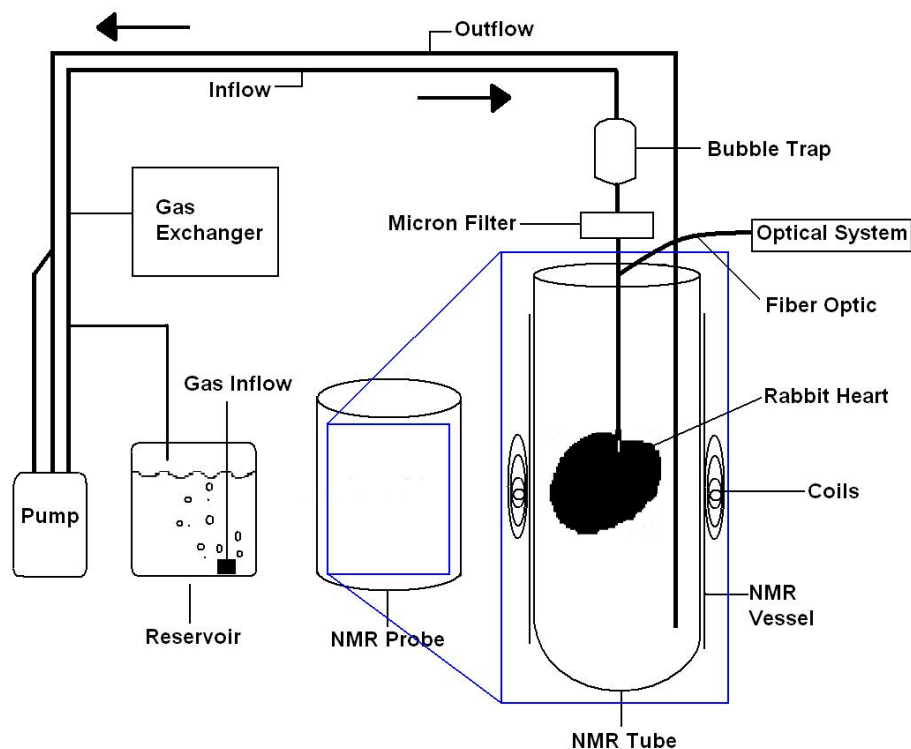


Figure 3.1. Diagram of the perfusion apparatus used in rabbits experiments.

The Tyrode solution perfusate was composed of the following (in mM): 129 NaCl, 5.4 KCl, 1.8 CaCl₂, 1.1 MgCl₂, 26 NaHCO₃, 1 Na₂HPO₄, and 11 glucose. The solution was equilibrated to 95% O₂ and 5% CO₂ with gas exchangers fabricated from silicone tubing. The hearts were placed in a standard 28-mm glass NMR tube with inflow and outflow tubes. The perfusate was delivered at a flow rate of 23 ml/min and at room temperature (23.5 °C) during all experiments. The outflow tube removed residual perfusate at a flow rate of 27 ml/min to avoid overflowing of the NMR tube. Throughout the procedure, the hearts were perfused with physiological saline except when attempting to induce ischemia. Hearts were stained with a stock solution of Di-4-ANEPPS (5mg Di-4-ANEPPS dissolved in 3mL of DMSO). The dye was loaded, by bolus injection of 0.4 ml stock solution, through the tubing above the aorta.

3.3 ^{31}P NMR and Optical Fluorescence Measurements

To record ^{31}P NMR spectra, the NMR tube was placed in a glass cradle of a custom-built ^{31}P NMR probe. Beforehand, the heart was positioned in the NMR tube to be aligned with the sweet spot of the ^{31}P Helmholtz coil, i.e. the spot where the sensitivity of NMR signal was greatest. The probe was placed in a Bruker Avance 360 MHz NMR spectrometer (80 mm vertical bore), and tuned and matched to 145.8 MHz, the ^{31}P resonance frequency. The field value and shim set remained consistent throughout the experiments. Spectra were acquired every 2 minutes by averaging 64 transients, each with 2 second duration.

To simultaneously record transmembrane APs, a custom optical fluorescence emission measurement system was used (Figure 3.2). Hearts were excited with blue argon laser light (488 nm) that passed through a fiber optic and was transferred to another fiber optic using a blue dichroic mirror. The light then passed through the fiber optic that was inserted into the aortic cannula of the perfusion system and into the left ventricle, exciting the fluorescent dye in ventricular endocardium. Emitted fluorescence from the heart was collected with the same fiber optic that delivered the excitation light. The light passed through filters, to separate the red and green fluorescence, and was collected by two photomultiplier tubes (PMTs). PMTs are extremely sensitive detectors of light. They take incident light photons, generate electrons by the photoelectric effect, and accelerate them through an electric field while contacting several dynodes. Upon striking each dynode, low energy electrons are released and progress towards the next dynode. PMTs output a voltage proportional to the number of initial photons. The gain can be adjusted by altering the dynode voltage. The PMTs produced two waveforms, red and

green, on an oscilloscope. Each of these represents the motion and action potentials produced by the heart. The ratio of the red and green signals from the PMTs was used to reveal APs without motion artifacts. Optical recordings of the APs were taken every 2 minutes, approximately 1 minute into each NMR spectral acquisition. Optical APs were observed and saved on an oscilloscope; NMR data were saved on the Bruker.

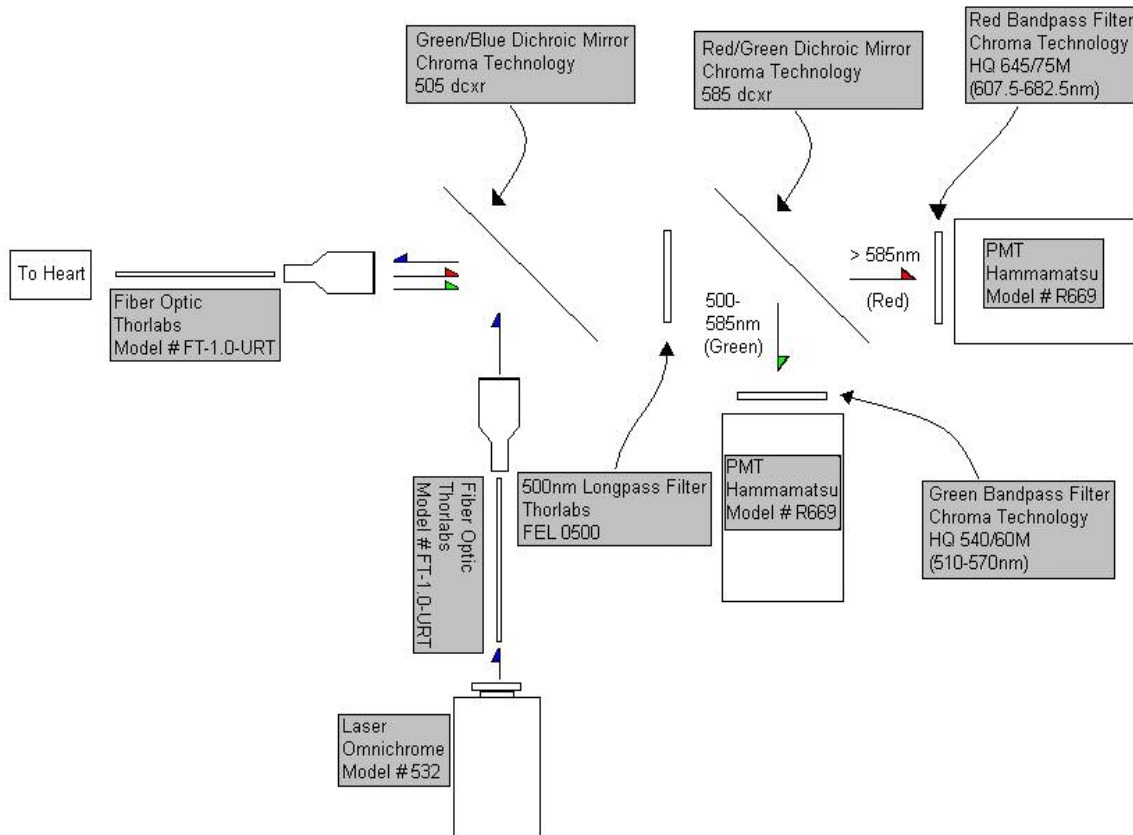


Figure 3.2. Optical recording system for ratiometric measurements in rabbit hearts stained with transmembrane voltage-sensitive fluorescent dye di-4-ANEPPS.

Simultaneous ^{31}P NMR and optical fluorescence measurements were first taken for 20 minutes during pre-ischemia/control. Ischemia was induced by interrupting the aortic perfusion at 20 minutes. Approximately half of the experiments maintained ischemic conditions for 10 minutes and the other half for 20 minutes. In all experiments,

reperfusion occurred directly after ischemia and measurements were taken for an additional 30 minutes.

CHAPTER IV

RESULTS

4.1 Overview

A total of five live rabbit experiments were completed over a 6 month period. However, due to the complexity of the dual modality system, only two of those experiments produced viable, simultaneous optical and ^{31}P NMR data. These two experiments were completed on August 2nd, 2005 and September 26th, 2005; henceforth, these two experiments will be designated as “Run #1” and “Run #2,” respectively. Both runs produced data in both modalities, however, Run #1 did not show any optical APs beyond the first control recording (as seen in Figure 4.1).

4.2 Optical Recordings in Control, Ischemia, and Reperfusion

Figure 4.1 shows ratiometric optical recordings of the APs during pre-ischemia of Run #1 and at key points during Run #2. Run #1 produced an excellent example of a control AP; however possible equipment malfunction reduced the remainder of the AP recordings to noise. Run #2 produced recordings that more closely resembled the morphology of an AP. (The viability of these recordings will be discussed further in the next chapter.) Run #1 recordings were taken with a ten second length while Run #2 recordings were taken with a four second length. The reduction in the length of recording was done to reduce save time. All optical recordings were also filtered with a 5 ms boxcar filter to eliminate high frequency noise.

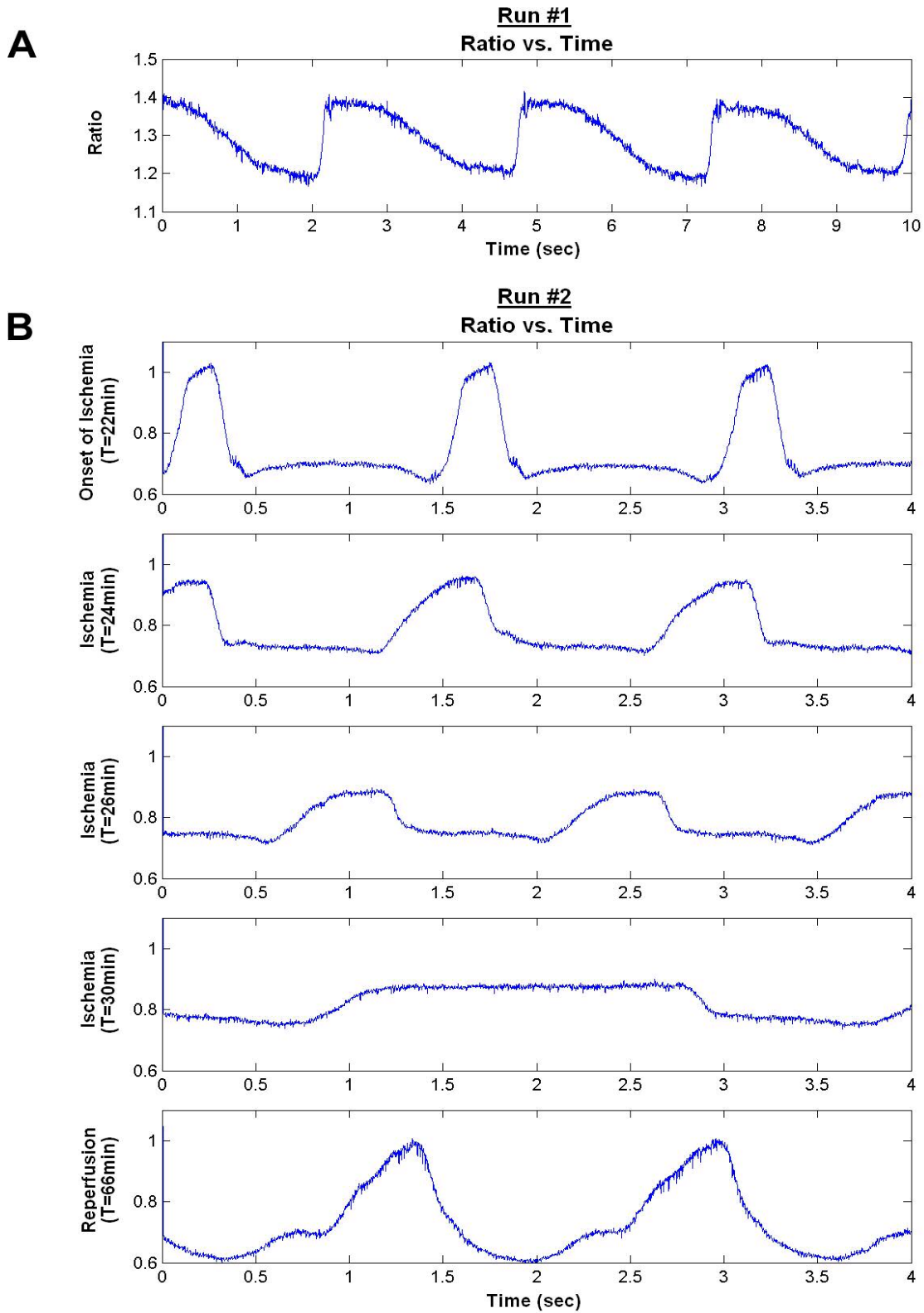


Fig 4.1. Ratiometric fluorescence recordings of action potentials (A) during pre-ischemia of Run #1 and (B) at key points during Run #2. Emission ratiometry techniques were used to produce the true action potential. A 5 ms boxcar filter was used. A boxcar filter is a digital FIR filter and thus has linear phase.

Figure 4.1 shows AP recordings at the onset of ischemia (approximately one minute into ischemia), at various points during ischemia, and approximately 15 minutes after reperfusion.

A boxcar filter is a digital FIR filter and thus has linear phase. Figure 4.2 shows the implementation of the boxcar filter and how it produces no phase change in the filtered result.

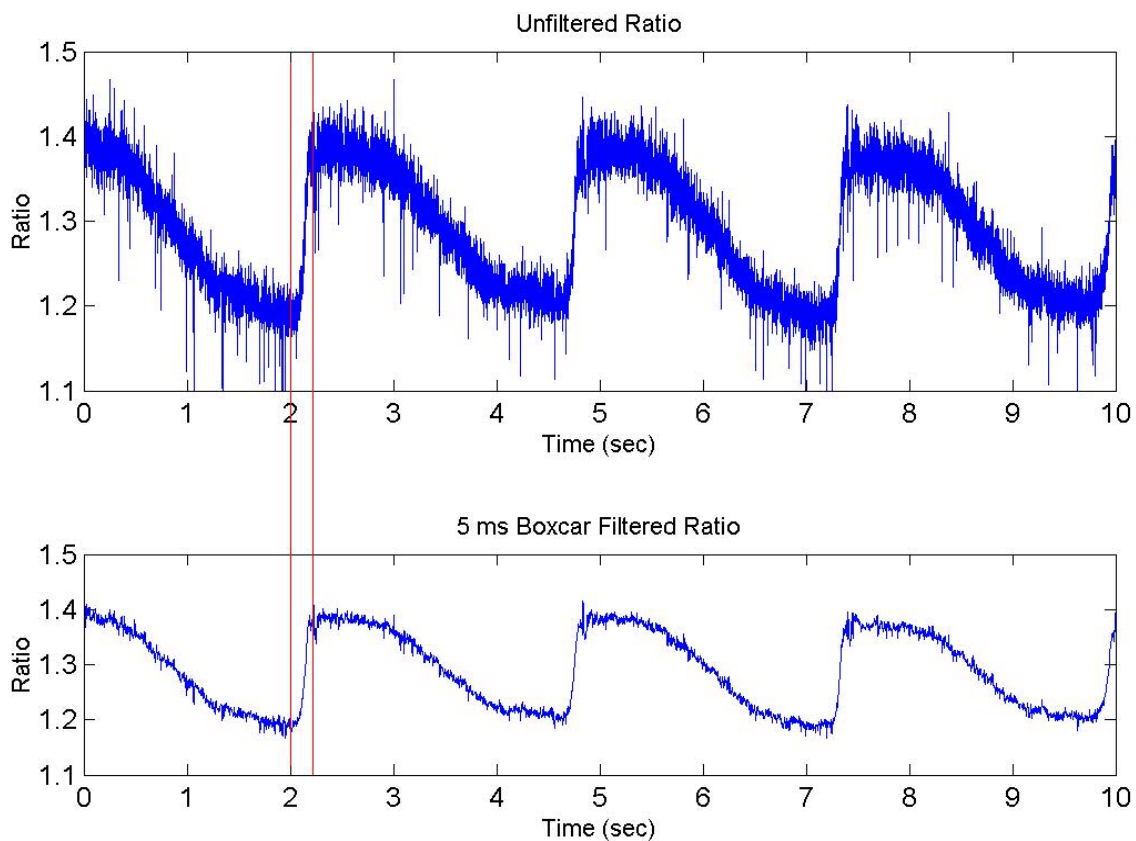


Figure 4.2. *Implementation of the 5ms boxcar filter. Comparing the unfiltered ratio with its filtered counterpart, it can be seen that there is no phase shift due to the implementation of the boxcar filter.*

Matlab was utilized to calculate standard aspects of AP morphology. Values for AP amplitude (APA), AP duration at 50% amplitude (APD_{50%}), and beats per minute (BPM) were calculated through graphical interpretation. APA was determined by

subtracting the baseline ratio value from the maximum value at the AP peak. $APD_{50\%}$ was calculated by subtracting the time from time at half the repolarization amplitude. BPM was determined by extrapolation from the number of APs that occurred during the four second period. A summary of these values are contained in Table 4.1.

Time	APA (unitless)	$APD_{50\%}$ (sec)	BPM (min^{-1})
22 minutes (Onset of Ischemia)	0.3	0.25	45
24 minutes (Ischemia)	0.2	0.308	40
26 minutes (Ischemia)	0.1	0.46	38
28 minutes (Ischemia)	0.08	1.85	24
30 minutes (Ischemia)	0.07	2	21
32 minutes (Ischemia)	0.09	>2	19.53
34 minutes (Ischemia)	0.07	>2	<19.53
36 minutes (Ischemia)	0.05	>2	<19.53
38 minutes (Ischemia)	0.05	>2	<19.53
40 minutes (Ischemia)	No Data	No Data	No Data
66 minutes (Reperfusion)	0.4	.38	40.05

Table 4.1. *Optical Action Potential Analysis for Run #2.*

At the time of ischemia (T=20min-40min), optical measurements show an overall reduction in APA by 83.3%, an increase in $APD_{50\%}$ by 875%, and reduction in intrinsic heart rate by 56.6% (Table 4.1). Ischemic recordings continued to follow this trend until perfusion was reinstated. Due to the increasing duration of the AP after 32 minutes and the short, four second recording period, it became impossible to determine the $APD_{50\%}$

and BPM. No optical data was collected for ischemia at the 40 minute mark due to equipment error.

4.3 ^{31}P NRM Spectroscopy Recordings in Control, Ischemia, and Reperfusion

Spectra were comprised of five phosphate peaks representing phosphocreatine, ATP (α , β , and γ), inorganic phosphate, and phosphomonoester (the latter two are usually interpreted as one peak). Once acquired, the spectra were adjusted by zero-order phasing (PH0) and automatic baseline subtraction (ABS). A standard NMR line-broadening factor of 30 Hz was applied in the frequency domain. The α -ATP peaks were calibrated to 7.5 ppm to match traditional ^{31}P NMR data presentation. By utilizing the Bruker's integration function, the area under each of the five peaks was determined. Individual phosphate levels in each spectrum were determined as a percentage of the total phosphate peak area for PCr, Pi, $\alpha/\beta/\gamma$ ATP, and phosphomonoesters (PME). Figure 4.3 are spectra from Run #1 during pre-ischemia, ischemia, and reperfusion.

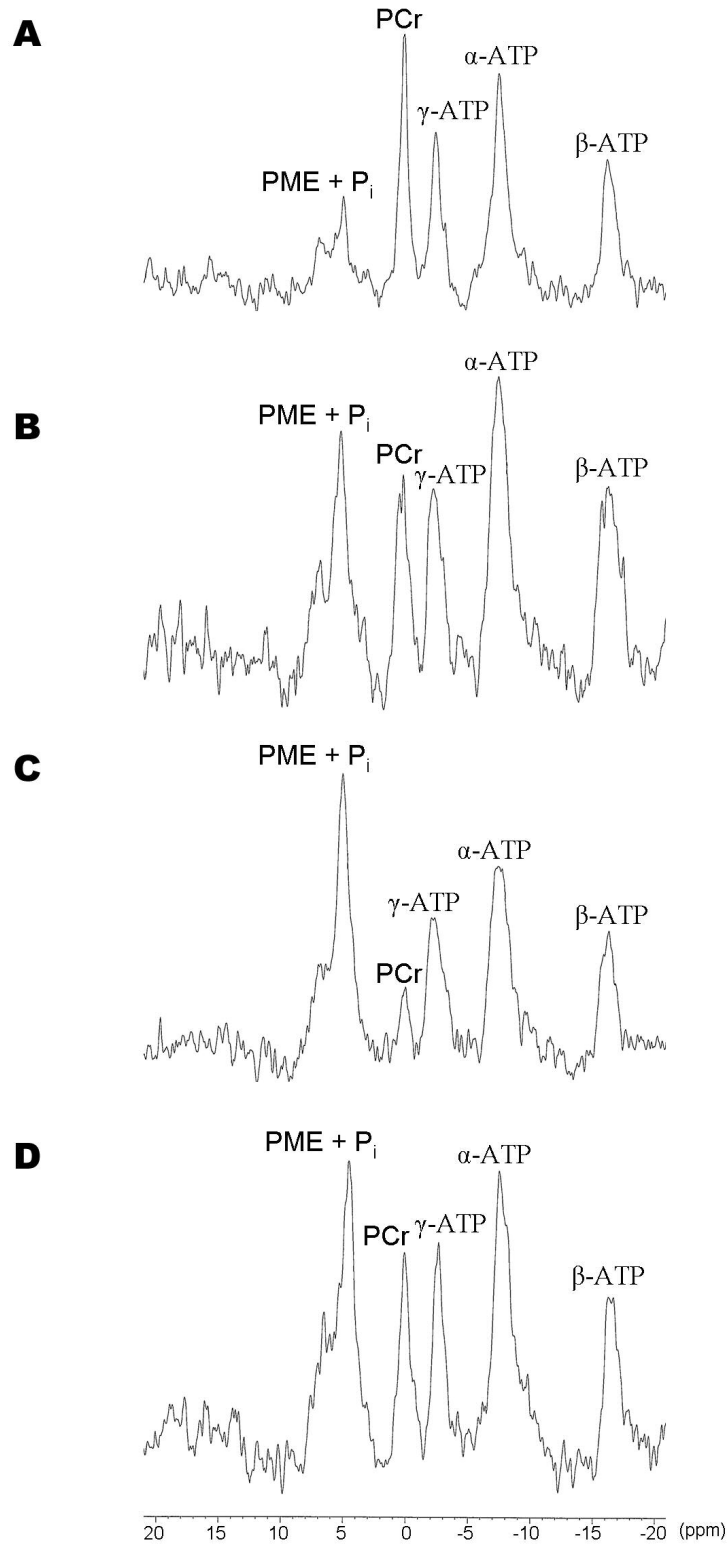


Fig 4.3. Representative ^{31}P NMR spectra from Run #1. Each spectrum shows five peaks and assigned as follows (from left): phosphomonoesters and inorganic phosphate (PME+P_i), phosphocreatine (PCr), α -adenosine triphosphate (ATP), β -ATP, and γ -ATP. (A) Control, pre-ischemia; (B) Two minutes into ischemia; (C) 10 minutes into ischemia; (D) 24 minutes after reperfusion.

4.4 Time Course of Phosphates and Intracellular pH

Individual phosphate levels in each spectrum were determined as a percentage of the total phosphate peak area for PCr, Pi, $\alpha/\beta/\gamma$ ATP, and phosphomonoesters (PME). Figure 4.4 shows analysis of phosphate levels before, during, and after ischemia for Run #1 and Run #2. In Run #1, acute ischemia was induced for 10 minutes while in Run #2, ischemia was induced for 20 minutes. Run #2 also provided a longer reperfusion period that seems to provide a more complete view of recovery.

The data conforms to previous findings concerning the stoichiometric relationship between inorganic phosphate and phosphocreatine; as phosphocreatine levels decrease, inorganic phosphate levels increase (Honda, Hajime et. al. 2002). Also as expected, β -ATP levels appear to decrease slightly during ischemia; however this decrease is small relative to changes in phosphocreatine and inorganic phosphate levels. In Run #2, reperfusion phosphate levels almost return to their pre-ischemia values. However, even after reperfusion, NMR data from Run #1 suggests the heart remains ischemic.

In Run #1, the difference between PCr levels at the pre-ischemia baseline and levels shortly before reperfusion is approximately 19% TP. Following the same process, the maximum change in Pi levels and β -ATP levels is approximately 20% TP and 4% TP, respectively. In Run #2, the maximum change in PCr, Pi, and β -ATP levels is approximately 19% TP, 35 %TP, and 3% TP, respectively.

Figure 4.5 shows the time course of pH levels during Run #1 and Run #2. The intracellular pH was determined by comparing the Pi chemical shift in each spectrum with the Pi chemical shift from a standard solution (Seo, Murakami et. al. 1983). Run #1 shows a decrease in pH from ≈ 7.1 to 6.8. Run #2 appears to have no change in pH.

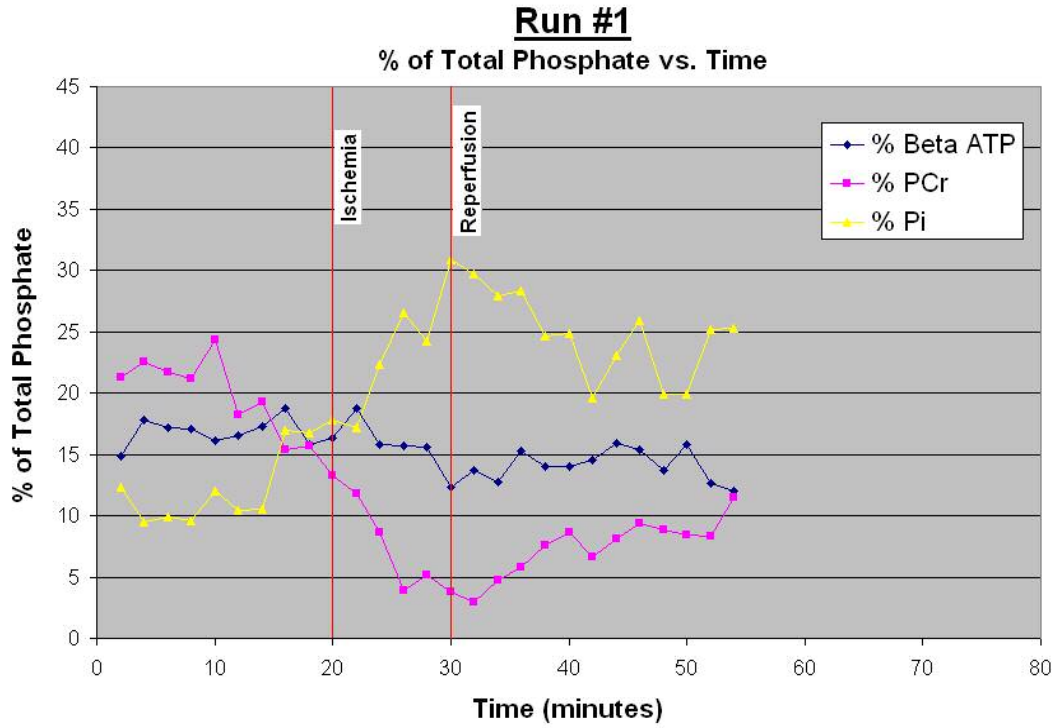
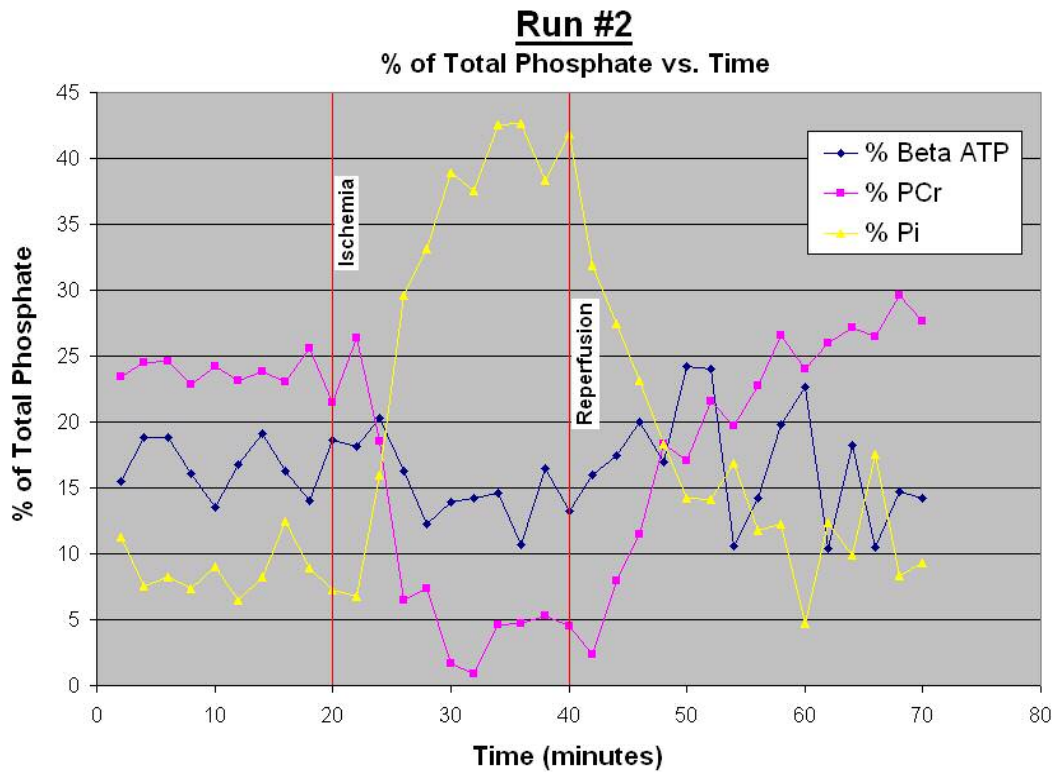
A**B**

Fig 4.4. Complete time course of changes in β -ATP, PCr, and Pi levels during (A) Run #1 and (B) Run #2. Ischemia was induced by turning off the perfusion apparatus at the 20-minute mark. Reperfusion of the rabbit heart occurred at the 30-minute mark in Run #1 and at the 40-minute mark in Run #2.

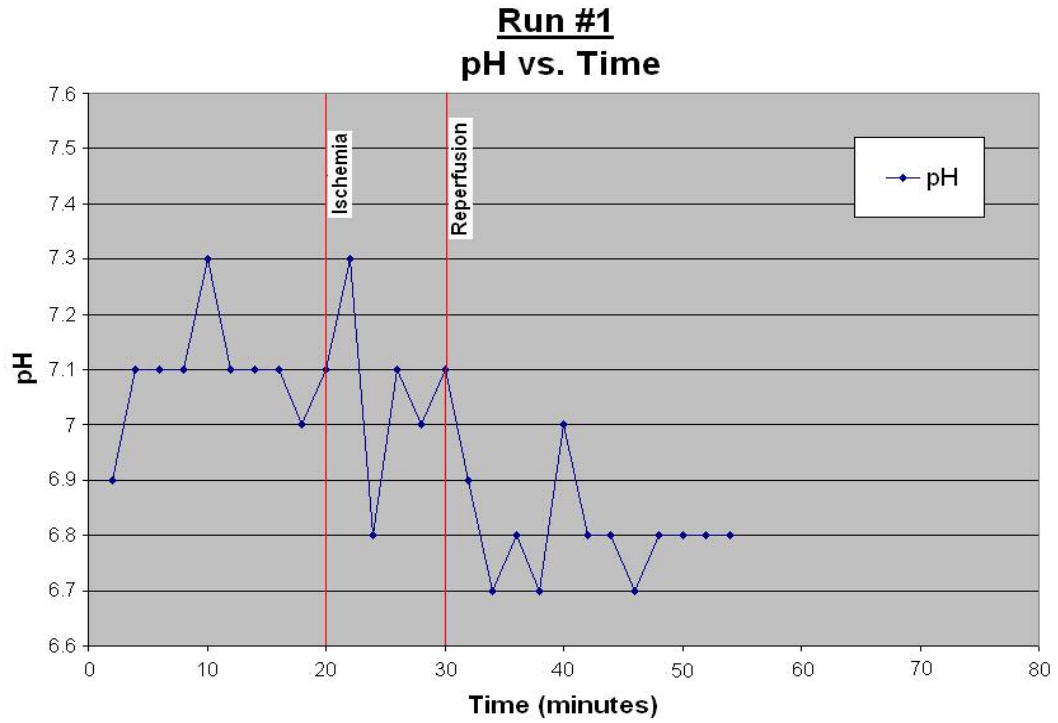
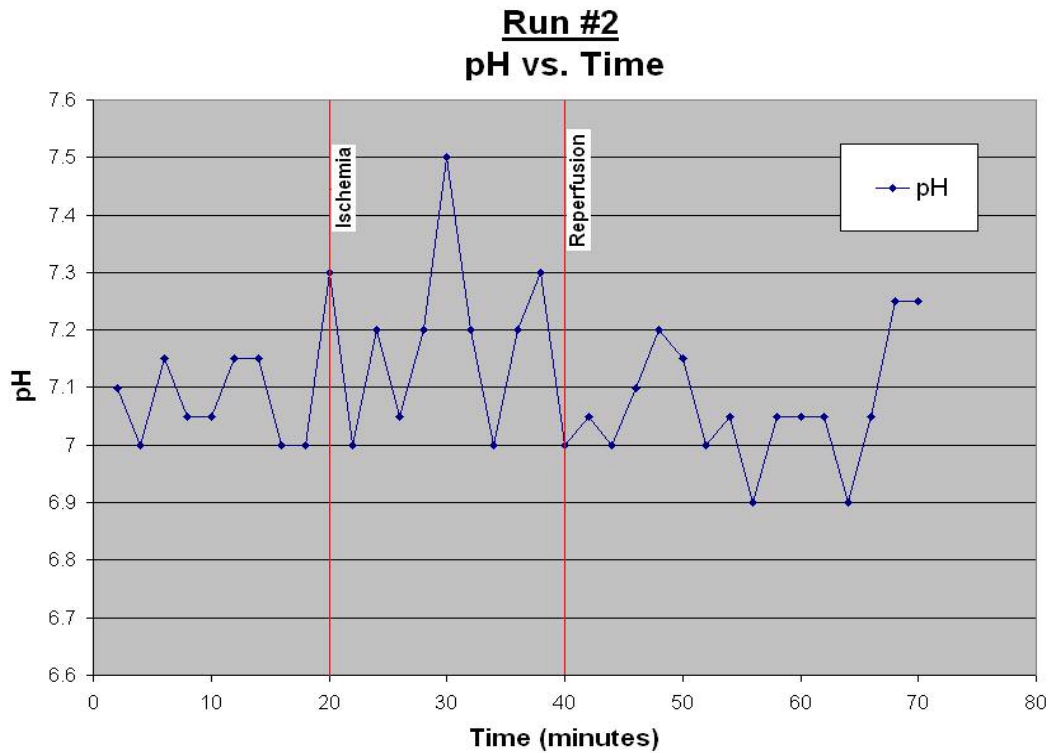
A**B**

Fig 4.5. Complete time course of changes in intracellular pH during (A) Run #1 and (B) Run #2.

CHAPTER V

DISCUSSION

5.1 Explanations for Abnormal Optical AP Morphology

There were two main concerns after analyzing the optical AP data in Run #2: (1) the prolonged action potential duration and (2) the lack of an obvious phase-zero depolarization. There are several explanations for the prolonged action potential duration. First, temperature can have a significant effect on AP characteristics. For example, decreased temperatures ranging from approximately 15–21°C can result in a heart rate of as little as a few BPM. Temperature affects the permeability of the cardiac myocyte membrane to the ions that are responsible for excitation. Higher temperatures provide increased permeability (i.e. rates at which channels open, close, and inactivate) and a higher level of excitability (Guyton, A. C. et. al. 2000). It is also a well-known fact that chemical reactions, i.e. metabolic processes, proceed at a faster rate with warmer temperatures. Considering all experiments were performed at a room temperature of approximately 23.5°C, it is expected that APD would increase due to slower changes in ionic currents. Therefore, the phase-zero depolarization, plateau, repolarization, etc. would all be prolonged. Kiyosue et. al. studied action potential prolongation at low temperatures in guinea-pig ventricular myocytes. They found that by reducing the temperature from 33-34°C to 24-25°C the APD increased by 115% (Kiyosue T. et. al.

1993). Knisley et. al. recorded normal optical APs at 35-36°C that were approximately 200 ms in duration with a setup similar to the one in this thesis (Knisley, S.B. et. al. 2000). Therefore, considering Run #1 produced AP recordings approximately 2 seconds in duration at 11°C colder, there seems to be other factors possibly involved in prolonging APD. Also, recall the conclusion that, during ischemia, AP duration is first prolonged and then shortens (Verkerk, Arie O., Veldkamp, Marieke W., et al. 1996). If temperature slows metabolic processes and the rate at which channels open, close, and inactivate, then 23.5°C might have been cold enough that AP duration had not yet reached the point where it begins to shorten. Therefore, low temperature might explain the fact that Run #2 had APs that continued to increase in duration.

Spatial averaging is another concept that might have influenced the apparent APD. When recording optical APs, our fiber optic's open end is placed firmly against the base of the ventricular endocardium. Girouard, S.D. et. al. introduced the idea that poor spatial resolution due to larger recording site areas can prolong the upstroke of an AP. They concluded that since the optical AP is derived from the average of all the single cell potentials in the volume under interrogation, it is possible that artifactual prolongation of the AP can skew recordings (Girouard, S.D. et. al. 1996).

Three other possibilities exist for prolonged APD. First, air bubbles might have been introduced into the coronary vessels during perfusion causing air emboli and local areas of ischemia before perfusion was terminated. Second, ischemia could have also been a result of damage to the heart during or after surgery. Prolonged periods without perfusion or low perfusate temperatures could have sent the heart into premature ischemia. Third, the optical signal contained both transmembrane APs and motion

artifacts due to the change in geometry when the heart contracts. Contraction may be slow when hearts are ischemic or cool, producing a large APD.

As for the apparent absence of phase-zero depolarization in the optical APs of Run #2, only two explanations are offered. First, the position of the fiber tip could have been altered by the movement of the heart during contraction. If the tip of the fiber optic lost contact with the left ventricular endocardium, there would be increased spatial averaging, increased motion artifacts, and changes in the green and red signal due to transmittance across air and perfusate. Second, extremely poor spatial resolution of the fiber optic could have distorted the phase-zero depolarization beyond recognition.

5.2 Viability of AP Recordings

In order to convincingly correlate the optical AP data with the NMR data, the viability of the optical AP recordings must be confirmed. Run #2 produced APDs that were more similar to expected values, but lacked the standard, characteristic AP morphology seen in Run #1's control recording. It can be argued that the optical AP recordings for Run #2 are viable based on two points: (1) even with abnormal characteristics, the optical recordings in Run #2 consistently follow the trends expected for AP morphology during ischemia; (2) and possibly the most compelling argument, raw oscilloscope measurements show electrical activity in the green and red recordings. Run #2 produced APDs that were more feasible, but unfortunately lacked the standard, characteristic AP morphology seen in Run #1's control recording.

The analysis of the characteristics of the optical AP recordings for Run #2 follows trends for previous findings concerning changes in AP morphology during ischemia. The APA decreases from 0.3 at the onset of ischemia to 0.05 before reperfusion (Hicks, M. N.

et. al. 1995). However, $APD_{50\%}$ shows an increase from 0.25 sec to at least 2 sec. Previous findings observed a short period of APD prolongation followed by APD shortening (Verkerk, Arie O., Veldkamp, Marieke W., et al. 1996). However, previously discussed low temperature concerns combined with ischemic conditions may have prolonged the period of APD prolongation. Also, delayed motion in ischemia may prolong the signal. Considering BPM data were calculated from the $APD_{50\%}$, the intrinsic heart rate appeared to decrease at least by 25.47 BPM. After approximately 15 minutes of reperfusion, APs showed a near full recovery of APA, $APD_{50\%}$, and BPM as expected in acute ischemia.

Figure 5.1 shows raw oscilloscope measurements from the green PMT and red PMT. The presence of electrical activity can be verified by searching for points where one signal is increasing in magnitude while the other signal is simultaneously decreasing, indicated by the red lines in the examples below. Run #2 confirms electrical activity; however possible malfunction in the PMT unit or unknown factors seem to have inverted or concealed it.

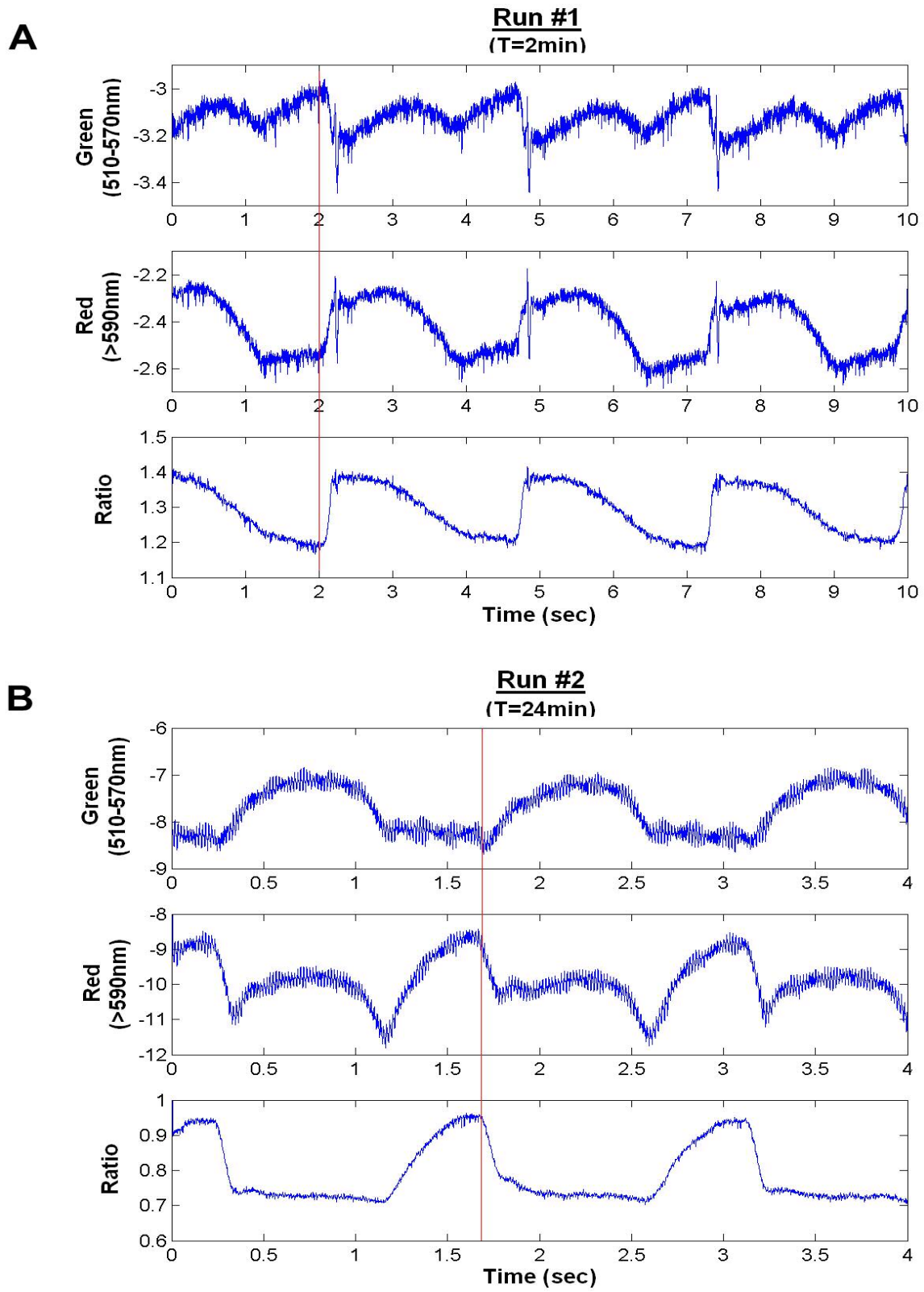


Figure 5.1. Fluorescence emission recordings for (A) Run #1 (pre-ischemia) and (B) Run #2 (approx. 4 min into ischemia). Red lines indicate phase-zero depolarization.

5.3 Simultaneous ^{31}P NMR and Optical Recordings of APs

During acute ischemia, several changes occur related to electrical activity and metabolism in the heart. As APA decreased and APD increased, PCr levels decreased and Pi levels increased. β -ATP levels slightly decreased as well, but the consumption of PCr stores and stimulation of the glycolytic pathway keep ATP levels relatively constant. (However, prolonged ischemia will eventually exhaust ATP stores.)

ATP consumption may have also indirectly prolonged the APD further. The production of free radicals is a normal by-product of ATP consumption. However, during ischemia, free radicals accumulate, along with lactic acid and Pi, because of the cardiac muscle's inability to eliminate them efficiently. Free radicals attack proteins and lipids, therefore, excessive amounts of free radicals can cause disturbances in ion permeation and the behavior of membrane channels (Carmeliet, Edward 1999). During acute ischemia, accumulated oxygen-derived free radicals increase APD by inhibiting resting K^+ leakage current and possibly altering the time-dependent currents of voltage-gated K^+ and Ca^{2+} channels (Jabr, R. I. and Cole, W. C. 1993).

During reperfusion, APA and APD returned almost to control levels. This coincided with the return of PCr and Pi to control levels as well. β -ATP levels recovered slower, as expected with longer periods of ischemia (Carmeliet, Edward 1999).

Run #1 appeared to have a decrease in pH levels over the course of the experiment. However, Run #2 had no apparent change in pH levels. This may be due to the ability of the heart from Run #2 to recover during reperfusion. Based upon the fact that PCr and Pi levels never returned to their original levels, it can be assumed that the

heart from Run #1 remained ischemic through reperfusion. Therefore, changes in pH might be more pronounced during longer periods of ischemia.

CHAPTER IV

CONCLUSIONS

Using the dual modality system, it was possible to simultaneously recorded cardiac optical APs and high-energy metabolite levels. Energy levels changed as expected while fluorescence showed decrease in heart rate and other characteristics of ischemia. For the first time to our knowledge, cardiac optical APs and high-energy metabolite levels are able to be recorded simultaneously and analyzed for correlation, providing a wealth of new insight into the relationship between cardiac metabolism and electrical activity.

Since fabrication, the system has been further optimized for improved performance. One of the goals of the current research was to improve upon the system even more, utilizing current results. Therefore, there are several improvements for future work. First, the heart temperature will be regulated and monitored during each experiment to ensure hearts remain at normal, physiological temperature. Second, the fiber optic tip will be properly secured against the left ventricular endocardium to resolve any issues with loss of contact. Third, the proper spatial area of the fiber optic tip will be determined for maximum spatial resolution. Fourth, the temporal resolution will be reduced further to attempt to observe faster changes in AP morphology and high-energy metabolite levels. Improving upon this system will provide future researchers with a powerful tool for correlating changes in cardiac electrical activity with metabolism.

REFERENCES

- Penny WJ and Sheridan DJ.** Arrhythmias and cellular electrophysiological changes during myocardial "ischemia" and reperfusion. *Cardiovasc Res* **17**(6): 363-72, 1983.
- Seo Y, Murakami M, Watari H, Imai Y, Yoshizaki K, Nishikawa H, and Morimoto T.** Intracellular pH determination by a ³¹P-NMR technique. The second dissociation constant of phosphoric acid in a biological system. *J Biochem (Tokyo)* **94**(3): 729-34, 1983.
- Knisley SB, Justice RK, Kong W, and Johnson PL.** Ratiometry of transmembrane voltage-sensitive fluorescent dye emission in hearts. *Am J Physiol Heart Circ Physiol* **279**(3): H1421-33, 2000.
- Kupriyanov VV, Dai G, Shaw RA, Sun J, Jilkina O, Luo Z, Mantsch H, and Deslauriers R.** Noninvasive assessment of cardiac ischemic injury using (87)Rb and (23)Na MRr imaging, (31)P MR, and optical spectroscopy. *Magn Reson Med* **44**(6): 899-908, 2000.
- Marsden PK, Strul D, Keevil SF, Williams SCR, and Cash D.** Simultaneous PET and NMR. *Br J Radiol* **75 Spec No**: S53-9, 2000.
- Tamura M, Hazeki O, Nioka S, and Chance B.** In vivo study of tissue oxygen metabolism using optical and nuclear magnetic resonance spectroscopies. *Annu Rev Physiol* **51**: 813-34, 1989.
- Tamura M, Hazeki O, Nioka S, Chance B, and Smith DS.** The simultaneous measurements of tissue oxygen concentration and energy state by near-infrared and nuclear magnetic resonance spectroscopy. *Adv Exp Med Biol* **222**: 359-63, 1988.
- Coronel R, Fiolet JW, Wilms-Schopman JG, Opthof T, Schaapherder AF, and Janse MJ.** Distribution of extracellular potassium and electrophysiologic changes during two-stage coronary ligation in the isolated, perfused canine heart. *Circulation* **80**(1):165-77, 1989.
- Carmeliet E.** Cardiac Ionic Currents and Acute Ischemia: From Channels to Arrhythmias. *Physiol. Rev* **79**: 917-1017, 1999.
- Verkerk AO, Veldkamp MW, van Ginneken AC, and Bouman LN.** Biphasic Response of Action Potential Duration to Metabolic Inhibition in Rabbit and Human Ventricular Myocytes: Role of Transient Outward Current and ATP-regulated Potassium Current. *J Mol Cell Cardiol* **28**(12): 2443-56, 1996.

- Clusin WT.** Calcium and cardiac arrhythmias: DADs, EADs, and alternans. *Crit Rev Clin Lab Sci* **40**(3): 337-75, 2003.
- Aiello EA, Jabr RI, and Cole WC.** Arrhythmia and Delayed Recovery of Cardiac Action Potential during Reperfusion after Ischemia. *Circ Res* **77**: 153-162, 1995.
- Luo CH and Rudy Y.** A dynamic model of the cardiac ventricular action potential. I. Simulations of ionic currents and concentration changes. *Circ Res* **74**(6): 1071-96, 1994.
- Dennis SC, Gevers W, and Opie LH.** Protons in ischemia: where do they come from; where do they go to? *J Mol Cell Cardiol* **23**: 1077–1086, 1991.
- Coraboeuf E, Deroubaix E, and Coulombe A.** Acidosis induced abnormal repolarization and repetitive activity in isolated dog Purkinje fibers. *J Physiol* **76**: 97–106, 1980.
- Braunwald E and Kloner RA.** Myocardial reperfusion: a double-edged sword?" *J Clin Invest* **76**(5):1713-9, 1985.
- Taniguchi J, Noma A, and Irisawa H.** Modification of the cardiac action potential by intracellular injection of adenosine triphosphate and related substances in guinea pig single ventricular cells. *Circ Res* **53**: 131-139, 1983.
- Weiss J and Shine K I.** Effects of heart rate on extracellular $[K^+]$ accumulation during myocardial ischemia. *Am J Physiol* **250**(Heart Circ. Physiol. 19): H982-H991, 1986.
- Tranum-Jensen J, Janse MJ, Fiolet WT, Krieger WJ, D'Alnoncourt CN, and Durrer D.** Tissue osmolality, cell swelling, and reperfusion in acute regional myocardial ischemia in the isolated porcine heart. *Circ Res* **49**: 364-381, 1981.
- Peuhkurinen K J.** Ischemic Heart Disease at the Cellular Level. *International Journal of Bioelectromagnetism* (2):1, 2000.
- De Weer P.** Axoplasmic free magnesium levels and magnesium extrusion from squid giant axons. *J Gen Physiol* **68**: 159-178, 1976.
- Guyton AC and Hall JE.** Textbook of Medical Physiology. Tenth Ed. Philadelphia: W. B. Saunders Company; 144-151, 2000.
- Kiyosue T, Arita M, Muramatsu H, Spindler AJ, and Noble D.** Ionic mechanisms of action potential prolongation at low temperature in guinea-pig ventricular myocytes. *J Physiol* **468**: 85-106, 1993.

- Hicks MN, McIntosh MA, Kane KA, Rankin AC, and Cobbe SM.** The electrophysiology of rabbit hearts with left ventricular hypertrophy under normal and ischaemic conditions. *Cardiovasc Res* **30**(2):181-6, 1995.
- Girouard SD, Laurita KR, and Rosenbaum DS.** Unique properties of cardiac action potentials recorded with voltage-sensitive dyes. *J Cardiovasc Electrophysiol* **7**(11): 1024-38, 1996.
- Honda H, Tanaka K, Akita N, and Haneda T.** Cyclical Changes in High-Energy Phosphates During Cardiac Cycle by Pacing-Gated ³¹P Nuclear Magnetic Resonance. *Circ J* **66**: 80-86, 2002.
- Jabr RI and Cole WC.** Alterations in electrical activity and membrane currents induced by intracellular oxygen-derived free radical stress in guinea pig ventricular myocytes. *Circ Res* **72**: 1229-1244, 1993.
- Fluhler E, Burnham VG, and Loew LM.** Spectra, membrane binding, and potentiometric responses of new charge shift probes. *Biochemistry* **24**: 5749-5755, 1985.
- Johnson PL, Smith W, Baynham TC, and Knisley SB.** Errors caused by combination of Di-4-ANEPPS and Fluo3/4 for simultaneous measurements of transmembrane potentials and intracellular calcium. *Ann Biomed Eng* **27**: 563-571, 1999.
- Zipes DP and Jalife J.** Cardiac Electrophysiology: From Cell to Bedside. Third Ed. Philadelphia: W. B. Saunders Company; 2000.
- Gadian DG, Hoult DG, Radda GK, Seeley PJ, Chance B, and Barlow C.** Phosphorous nuclear magnetic resonance studies on normoxic and ischemic cardiac tissue. *Proc Natl Acad Sci* **73**(12): 4446-4448, 1976.